Experimental study of linear magnetic dichroism in photoionization satellite transitions of atomic rubidium

K. Jänkälä,[1,*] M. Alagia,[2] V. Feyer,[3] K. C. Prince,[3,2] and R. Richter[3]
[1]*Department of Physics, P.O. Box 3000, 90014 University of Oulu, Oulu, Finland*
[2]*CNR-IOM, Laboratorio TASC, IT-34149 Trieste, Italy*
[3]*Sincrotrone Trieste, Area Science Park, IT-34149 Trieste, Italy*
(Received 11 October 2011; published 22 November 2011)

Laser orientation in the initial state has been used to study the properties of satellite transitions in inner-shell photoionization of rubidium atoms. The linear magnetic dichroism in the angular distribution (LMDAD) has been utilized to probe the continuum waves of orbital angular momentum conserving monopole, and angular momentum changing conjugate satellites, accompanying the $4p$ ionization of atomic Rb. We show experimentally that LMDAD of both types of satellite transitions is nonzero and that LMDAD of monopole satellites, measured as a function of photon energy, mimics the LMDAD of direct photoionization, whereas the LMDAD of conjugate transitions deviates drastically from that trend. The results indicate that conjugate transitions cannot be described theoretically without explicit inclusion of electron-electron interaction. The present data can thus be used as a very precise test of current models for photoionization.

DOI: 10.1103/PhysRevA.84.053426 PACS number(s): 32.80.Fb, 32.80.Xx, 32.70.−n

I. INTRODUCTION

Photoionization "shake" satellites are caused by many-electron processes where a bound electron changes its single-electron orbital during the ionization of another electron. Spectral lines caused by satellite transitions are typically well separated from the main lines where one electron is ejected into the continuum while the other electrons remain in their initial orbitals. Photoionization satellites can be effectively used to probe the behavior of bound electrons in light-matter interactions. Therefore, since the 1960s numerous experimental and theoretical investigations of photoionization satellites have been published (see Refs. [1–19] and references therein).

Satellite transitions can be divided into two categories,[1] so-called monopole and conjugate satellites. In monopole satellites the orbital angular momentum of the shaken electron is conserved in the transition, and in conjugate satellites it changes (usually by ± 1). Therefore, for the monopole transitions the parity of the remaining ion is the same as for the direct ionization, and for the conjugate satellites the parity is opposite.

Monopole satellites are understood to arise from a sudden change of electric potential caused by removal of an electron [1,2,9]. This leads to a rapid rearrangement of the electron cloud. During this process an electron (usually in the valence) has a finite probability to "jump" from one single-electron orbital to another, while conserving its angular momentum. Monopole satellites can therefore be treated without including explicit electron-electron interaction. In this so-called sudden approximation, one electron absorbs the incoming photon and the second electron simply reacts independently to the change of the electric potential. Conjugate satellite transitions are considerably more demanding to describe, and in the past different approaches have been introduced. These include the sudden approximation [7,13,15,16,20], random-phase approximation with exchange [11,18], perturbation theory [4,6,10,11], and the R-matrix method [5,19,21,22]. However, despite decades of research, agreement between the experiment and theory of conjugate satellites is still often considerably worse than for the main lines and monopole satellites.

Magnetic dichroism in atomic systems is observed when the inherently random population of degenerate magnetic substates of an atomic ensemble is altered. More precisely, linear magnetic dichroism in the angular distribution (LMDAD) is defined as the difference between the partial cross section of two target orientations, provided that the ionizing radiation is linearly polarized [23]. The population of substates can be altered by pumping the atomic sample with circularly polarized laser light. Excitation with right-handed polarized light raises the magnetic quantum number of an atom by $+1$, and left-handed lowers it by -1.

LMDAD has been used to study several atomic elements and it has provided rich information about electron correlations and photoionization dynamics (see, e.g., reviews [24–26] and Refs. [27–32]). As an example, in conjunction with linear alignment dichroism in angular distribution (LADAD) it can be used to obtain values for the phase difference and amplitude ratio between the partial photoelectron continuum waves [28]. The behavior of LMDAD alone also provides valuable information. The information is similar to that obtained from the angular distribution of photoelectrons; thus, it is an effective test of subtle details of the photoionization dynamics [26]. The zero crossings of the profile are connected to the zeros of the phase difference of the continuum waves and to the Cooper minima [31,32]. In the case of weak lines, reliable measurement of photoelectron angular distributions can be a very demanding task due to the calibrations required and possibly the need of rotating a heavy vacuum chamber. The measurement of LMDAD, on the other hand, requires only a change of the helicity of the laser beam by turning the polarizing optics.

*kari.jankala@oulu.fi
[1]We distinguish shake satellites from configuration mixing lines that are not considered here.

In the present paper we describe an LMDAD study of photoionization satellites accompanying $4p$ photoionization of Rb as a function of photon energy. Previous studies utilizing dichroism to probe the dynamics of photoionization satellites are scarce. LADAD has been studied in shake-down satellites of aligned Na atoms at a single photon energy [33], and very recently Meyer *et al.* reported a surprising observation of nonzero LADAD and LMDAD in satellite lines of $1s$ ionization of laser excited Li [19]. In this paper we study monopole shake-up (MSU), conjugate shake-up (CSU), and conjugate shake-down (CSD) transitions from oriented Rb($4p^6 5s$) and Rb($4p^6 5p_{1/2}$) initial states to Rb($4p^5 5s$), Rb($4p^5 6s$), and Rb($4p^5 5p$) final ionic states. We show that LMDAD of all the satellite transitions is nonzero and that LMDAD of weak satellite transitions can be determined with high accuracy, which is useful for comparison to theoretical models. As a main result, we show experimentally that in conjugate satellite transitions two partial photoelectron continuum waves with different orbital angular momenta can be present. The result is very important in the development of models for conjugate satellites and double photoionization (DPI). It also proves that the commonly used sudden approximation model does not fully describe conjugate transitions.

II. EXPERIMENT

The experiment was carried out at the Gas Phase beamline [34] of the third-generation synchrotron radiation source Elettra, Trieste, Italy. The storage ring was running in multibunch, top-up mode with a constant current of about 300 mA. The laser used was a mode-locked Ti:Sa oscillator Tsunami made by Spectra Physics. The laser provided pulses of 15 ps at a repetition rate of about 83 MHz, with an average power of 1 W measured at the entrance of the experimental chamber. The laser was tuned to the Rb($5s \rightarrow 5p_{1/2}$) resonance at about 795 nm [35]. It was not synchronized to the synchrotron ring because the lifetime of the Rb($5p\,^2P_{1/2}$) state is long ($\sim$28 ns [35]) in comparison to the laser pulse period and the repetition rate of the synchrotron. For further details of the laser setup, we refer the reader to [36,37]. The laser polarization was set to circular using a combination of $\lambda/2$ and $\lambda/4$ plates. The quality of the polarization was also checked prior to measurement.

The electron spectra were measured using a hemispherical electron energy analyzer (VG) placed at the so-called magic angle of 54.7° with respect to the polarization vector of the linearly polarized synchrotron radiation. This angle is particularly useful in LMDAD measurements because the contribution from the standard angular anisotropy (specified by β parameter) vanishes. The measurements were carried out at constant pass energy of the analyzer. The total resolution including the photon energy bandwidth and Doppler broadening was about 100 meV. The Rb vapor was generated using a resistively heated oven at a temperature of 115 °C, which was monitored using a thermocouple. The laser beam was not focused, yielding a beam of approximately 2 mm diameter at the interaction region, which is about the size of the effusive Rb beam from the oven. The diameter of the laser beam was large compared to the synchrotron beam ($\sim$0.4 mm), so the variations in the overlap between the laser and synchrotron beams were negligible. The experimental conditions were observed to be very stable during the measurement period.

III. RESULTS

In the present study the total angular momentum of the ground and laser excited state is $J = 1/2$. Therefore, no more than half of the atoms in the interaction region can be excited by the laser and an ensemble of atoms in the ground state is always present. Circularly polarized laser light can excite only $M = \pm 1/2 \rightarrow M = \mp 1/2$ transitions and stimulated emission is forbidden. Because of this, laser pumping with right-handed (left-handed) laser light leads to increased population of atoms in the $M = +1/2$ ($M = -1/2$) magnetic substates in both the ground and the excited state, and all lines seen in the spectrum may display LMDAD. The laser helicity dependent direction of orientation is thus the same for both states, but the degree varies so that the ground state is slightly less oriented than the excited state. Figure 1 shows the $4p$ photoelectron spectrum of Rb measured at 45-eV photon energy. Dashed and dotted lines are measurements with the exciting laser light at two helicities. The solid line depicts the spectrum without laser. The energies of the final states that are of interest in the present study are marked, especially LSJ terms of the fine-structure lines for which LMDAD is determined are given.

The structures of interest in the photoelectron spectrum in Fig. 1 are described as follows. At low binding energy, CSD lines (magnified by 100) due to transitions from the $4p^6 5p_{1/2}$ initial state to the $4p^5 5s$ final states are seen. They are shifted toward lower binding energy by the energy of the laser photon, with respect to the main lines of atoms in the $4p^6 5s$ ground state. The main lines are followed by spectral structures corresponding to direct $4p$ ionization from the $4p^6 5p_{1/2}$ initial state. At higher binding energy a rich CSU satellite structure from both initial states is seen. Unfortunately, considerable overlap renders most of the lines unusable for LMDAD studies. This is partly due to the lines that correspond to ionization into the $4p^5 4d$ final states, which can also be found in this binding energy region [35]. Despite overlap, the LMDAD for two CSU lines ($^3P_0$ and $^3D_1$ final states) was determined. At the highest binding energy shown, lines corresponding to MSU into $4p^5 6s$ final states are shown.

Figure 2 shows LMDAD of the states marked in Fig. 1 as a function of photon energy. The relative LMDAD shown in Fig. 2 is defined as [23]

$$\beta_{\mathrm{LMDAD}} = \frac{I_+ - I_-}{I_+ + I_-}, \tag{1}$$

where I_+ and I_- are the observed electron intensities when the orientation of the initial states is produced by right-handed and left-handed circularly polarized light, respectively.

In panels (a)–(c) of Fig. 2, the angular momentum coupling of the final ionic states is identical. The difference between Figs. 2(a) and 2(b) is that in the final state the principal quantum number n of the outermost electron is 5 in Fig. 2(a) and 6 in Fig. 2(b). On the other hand, in Figs. 2(a) and 2(c) the final states are identical ($4p^5 5s$), but the parities of the initial states are opposite and the orbital angular momentum of the outermost electron is 0 in Fig. 2(a) and 1 in Fig. 2(c).

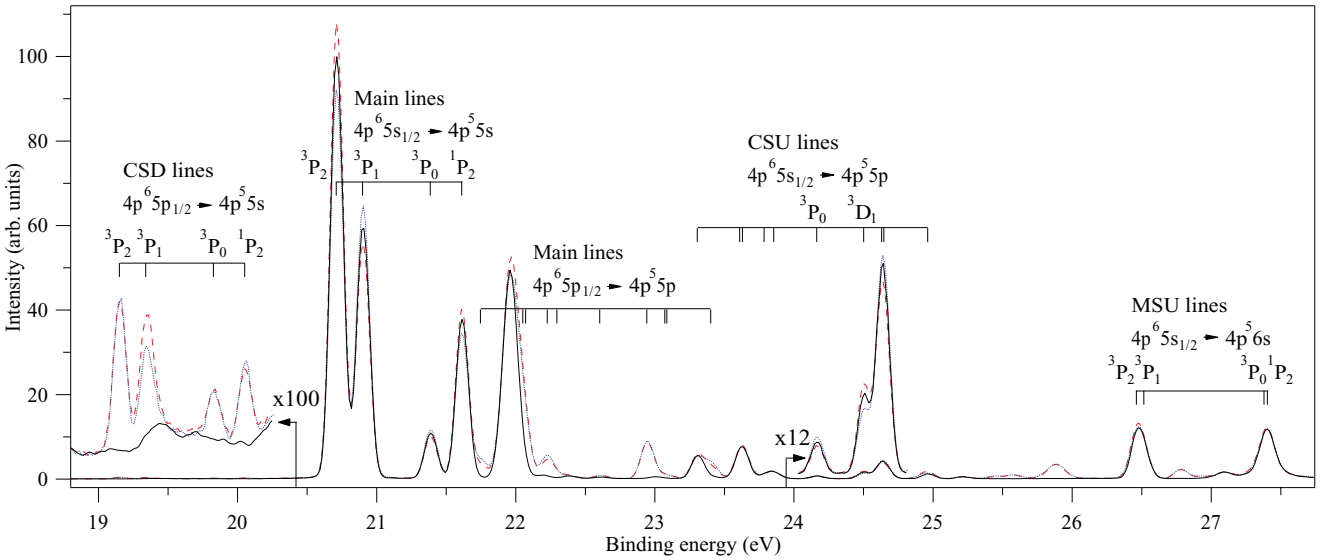

FIG. 1. (Color online) Experimental $4p$ photoelectron spectrum of atomic Rb measured at photon energy 45 eV. Dashed (red) curve, measurement with the pump laser light right-handed circularly polarize; dotted (blue) curve, left-handed circularly polarized; solid (black) curve, measurement without laser. Line assignments and energies are taken from the NIST database [35].

For comparison, Fig. 2(d) shows LMDAD of two lines that correspond to CSU transitions to $4p^5 5p$ final states from the ground state.

IV. DISCUSSION

The differential photoionization cross section can be written in the general form [38]

$$\frac{d\sigma}{d\Omega} = \frac{\sigma^{\rm iso}}{4\pi}\left[1 + \sum_{k_0 k k_\gamma} \mathcal{A}_{k_0 0}\beta_{k_0 k k_\gamma} F_{k_0 k k_\gamma}\right], \tag{2}$$

where $\sigma^{\rm iso}$ is the angle-integrated total photoionization cross section and $\mathcal{A}_{k_0 0}$ are the reduced statistical tensors of the initial state. The terms $F_{k_0 k_\gamma k}$ are geometrical factors that contain the information about the directions of atomic polarization and electron emission as well as the polarization of the incoming photon. The terms $\beta_{k_0 k_\gamma k}$ are the general anisotropy coefficients defined as [31,38]

$$\beta_{k_0 k k_\gamma} = \frac{3\hat{J}_0}{N}\sum_{l l' j j' J J'} (-1)^{J+J_f+k_\gamma-\frac{1}{2}}\hat{J}\hat{J}'\hat{j}\hat{j}'\hat{l}\hat{l}'\langle l0l'0|k0\rangle \times \begin{Bmatrix} j & l & \frac{1}{2} \\ l' & j' & k \end{Bmatrix}\begin{Bmatrix} j & J & J_f \\ J' & j' & k \end{Bmatrix}\begin{Bmatrix} J_0 & 1 & J \\ J_0 & 1 & J' \\ k_0 & k_\gamma & k \end{Bmatrix} \times M_{ljJ}M^*_{l'j'J'}, \tag{3}$$

where $M_{ljJ} = \langle \alpha_f J_f, lj : J\|\mathcal{H}\|\alpha_0 J_0\rangle$ is the reduced matrix element that describes a transition from the $|\alpha_0 J_0\rangle$ initial state to the $|\alpha_f J_f\rangle$ final ionic state with the emission of an electron of angular momenta l and j. The normalization is defined as $N = \sum_{ljJ}|M_{ljJ}|^2$. Equations (2) and (3) are valid for any (one-electron) photoionization process as long as the transition operator $\mathcal{H}$ in M_{ljJ} can be expressed in a spherical tensorial form.

If $\beta_{\rm LMDAD}$ is measured at the magic angle, the linearly polarized ionizing photon beam is collinear with the circularly polarized laser beam and the total angular momentum of the initial state J_0 is 1/2, then using Eqs. (1) and (2), the LMDAD signal can be cast in the form [23]

$$\beta^{54.7^\circ}_{\rm LMDAD} = -i\sqrt{\frac{15}{4}}\mathcal{A}_{10}\beta_{122}\sin 2\theta, \tag{4}$$

where θ is the magic angle. The term $\mathcal{A}_{10}$ acts only as a photon-energy-independent scaling factor, and thus the behavior of the LMDAD signal as a function of photon energy depends only on the β_{122} coefficient. The difference in comparison to the studies of the angular anisotropy is that instead of the β_{022} parameter, the β_{122} parameter is measured.

In the case of direct ionization from an np orbital, Eq. (4) can be further simplified to the form [28,39]

$$\beta^{54.7^\circ({\rm Dir})}_{\rm LMDAD} = C(\alpha_f, J_f)\frac{x}{x^2+1}\sin(\delta_s - \delta_d), \tag{5}$$

where $C(\alpha_f, J_f)$ contain the angular momentum coupling coefficients, $x = |D_s|/|D_d|$, and δ_l is the phase of the continuum wave. $D_l = \langle \epsilon l|\hat{D}|4p\rangle$ is a one-electron dipole matrix element. Equation (4) shows that the nodes of LMDAD profiles are observed if $D_s = 0$, $D_d = 0$, or $\delta_s - \delta_d = n\pi$ (where n is an integer) and the changes as a function of energy depend on the dynamics of photoionization.

The observed behavior of the LMDAD of the main lines in Fig. 2(a) can be understood within the framework of Eq. (5). The $C(\alpha_f, J_f)$ coefficients are the same for $^3P_2$ and $^1P_1$ final states and $^3P_1$ and $^3P_0$ final states. A simple calculation for the continuum waves, where the wave functions are solved directly from the Schrödinger equation in a fixed potential of the Rb ion, confirms that the node at 37-eV photon energy in Fig. 2(a) is due to the vanishing of the $\sin(\delta_s - \delta_d)$ term at around 15.6-eV photoelectron kinetic energy. The deviations between LMDADs of $^3P_2$ and $^1P_1$, and $^3P_1$ and $^3P_0$ states close to threshold can be understood by the binding energy

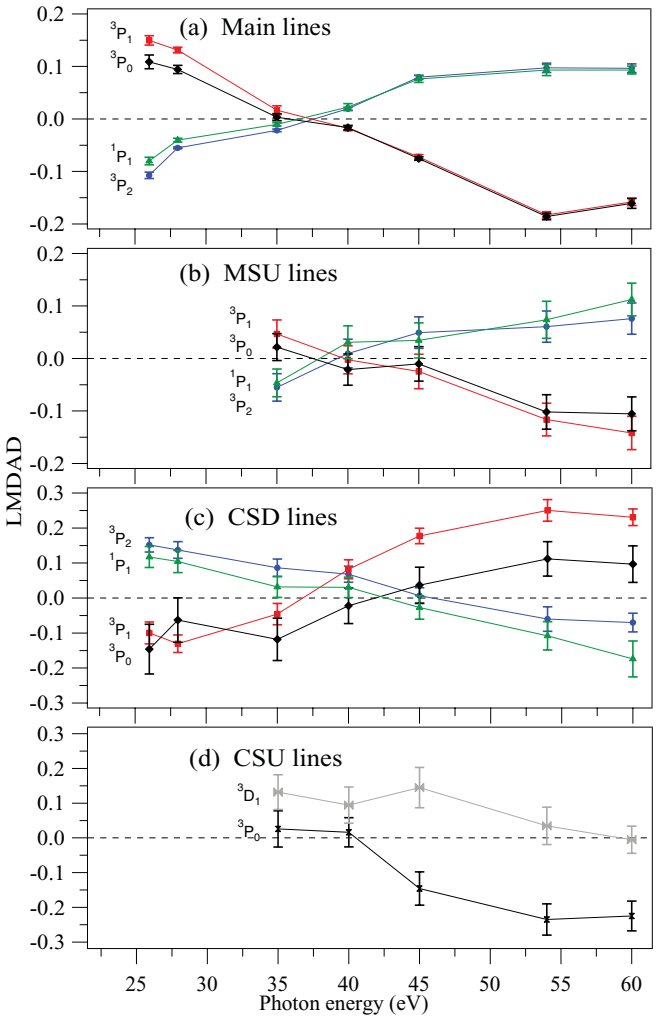

FIG. 2. (Color online) Experimental relative LMDAD as a function of photon energy at the interval 25–60 eV. Panel (a) shows the result for $4p^6 5s \rightarrow 4p^5 5s$, (b) for $4p^6 5s \rightarrow 4p^5 6s$, (c) for $4p^6 5p_{1/2} \rightarrow 4p^5 5s$, and (d) for $4p^6 5s \rightarrow 4p^5 5p$ ionization. LSJ terms mark the final ionic fine-structure states.

difference between the states and the slightly different potential felt by the outgoing photoelectron. We note that the profile also has a second node at 72-eV photon energy, which is due to vanishing of the D_s matrix element [32]. The data in Fig. 2(a) can be used as a very precise test of the quality of the calculated continuum wave functions in direct photoionization.

Figure 2(b) shows the LMDAD of $4p^6 5s \rightarrow 4p^5 6s$ MSU lines. The behavior can be explained using the sudden approximation model. Within this shake model, the one-electron photoionization MSU matrix elements are $D_l = \langle 6s|5s\rangle\langle \epsilon l|\hat{D}|4p\rangle$ ($l = 0,2$), and all angular momentum couplings are exactly the same as for the direct ionization in Fig. 2(a). Equation (5) can therefore be directly applied also to the present MSU case. Comparison between the LMDAD profiles in Figs. 2(a) and 2(b) shows that they are indeed very similar. The only significant difference is that in the MSU case, the zero crossings are found at higher photon energy. The difference is explained by the higher binding energy of the MSU states in comparison to the direct ionization. As an example, at the same photon energy the kinetic energy of a photoelectron connected to the $4p^5 6s\,^3P_2$ final state is about 5.75 eV smaller (see Fig. 1) than the kinetic energy of a photoelectron, leading to the $4p^5 5s\,^3P_2$ state.

As a last case the LMDAD of conjugate satellite transitions is studied. The profiles of the CSD and CSU transitions are shown in Figs. 2(c) and 2(d). Applying the sudden approximation to the CSD transitions in Fig. 2(c), the one-electron matrix elements are written as $D_p = \langle \epsilon p|4p\rangle\langle 5s|\hat{D}|5p\rangle + \langle \epsilon p|5p\rangle\langle 5s|\hat{D}|4p\rangle$. This kind of approximation has been used in many studies with varying success [7,9,11–13,15,16,20]. However, in this model only one partial continuum wave is possible, which is the p wave. If Eq. (4) is reduced into form (5) with a single p wave, the result is exactly zero at all photon energies. Therefore, the sudden approximation applied to conjugate transitions does not predict LMDAD. In contrast, the experimental data in Figs. 2(c) and 2(d) shows strong LMDAD for both CSU and CSD transitions. We note that in the relativistic formalism of the sudden approximation, $\epsilon p_{1/2}$ and $\epsilon p_{3/2}$ continuum waves are possible, but the phase difference between the waves is too small to explain the magnitude of the experimentally observed LMDAD. Also, initial-state electron correlation providing f waves is not likely to explain the effect because (in a first approximation) considerable $5p$-$4f$ mixing would be required. The presence of such mixing was ruled out by a calculation using Cowan's code [40].

Comparison of Figs. 2(a) and 2(c) yields fascinating results. First of all, the overall sign of LMDAD in Fig. 2(c) is inverted compared with Figs. 2(a) and 2(b). The most logical explanation is that the inversion arises from the angular momentum coupling due to change in the orbital angular momentum of the initial state. Thus, we infer that the change is due to geometrical factors and is not directly related to the dynamics of the transition. More interestingly, as in the case of direct ionization and MSU, the LMDAD curves of $^3P_2$ and $^1P_1$, and $^3P_1$ and $^3P_0$ final states do not converge to the same values in the photon energy interval considered. Also, the nodes of the LMDAD profiles of different final states are not found at the same kinetic energy. As an example, the energy difference between the zero crossing of LMDADs of $^3P_2$ and $^3P_1$ final states is about 3.2 eV, which is considerably larger than the binding energy difference 0.2 eV of these states. Because of this, LMDAD of these final states is about the same (and clearly nonzero) at the photon energy of 40 eV. Such behavior is not observed in the case of direct ionization (see also [32]). The observations indicate that electron correlation effects are very important in understanding CSU and CSD transitions. The fact that the nodes of the LMDAD profiles of conjugate satellite transitions in Figs. 2(c) and 2(d) are found at different kinetic energy positions is a strong indication that the transitions are described by varying combinations of continuum waves. Therefore, a successful theory of the LMDAD of conjugate transitions cannot be cast in a simple form similar to Eq. (5).

As discussed above, the sudden approximation cannot describe conjugate transition alone, because at least two partial continuum waves with different orbital angular momenta are present in the transition. A model providing this can be composed using, for example, perturbation theory, which allows the transition matrix elements to be written including

the electron-electron interaction explicitly. The approach has been used to describe DPI [41–43] and has been named internal electron scattering and direct knockout by some authors. The model has also been used in some studies of conjugate satellites (e.g., Refs. [4,6,10,11]), but hitherto not confirmed to be essential for a proper description. The model gives essentially similar matrix elements as continuum configuration interaction [8] used in Ref. [19] to describe dichroism effects in Li. The schematics of the model can be written as follows. Expanding the perturbation theory to second order, the photoionization matrix elements take a form

$$M_{i\to f} = \langle f|\hat{D}|i\rangle + \sum\!\!\!\!\!\!\int \frac{\langle f|\hat{U}|q\rangle\langle q|\hat{D}|i\rangle}{\omega - \epsilon_q + \epsilon_i + i\delta}, \tag{6}$$

where the first term on the left-hand side is the direct ionization (i.e., the sudden approximation) and the second term is a virtual Auger channel. The second term includes the sum and integral over all discrete and continuum intermediate states $|q\rangle$ and $\hat{U}$ is the Coulomb interaction operator. The matrix elements in the present case can be written as $\langle f|\hat{U}|q\rangle\langle q|\hat{D}|i\rangle = \langle 4p^5 5s;\, \epsilon\, l\,|\,\hat{U}\,|\,4p^5 5p;\, \epsilon\, l'\rangle\,\langle 4p^5 5p;\, \epsilon\, l'\,|\hat{D}|4p^6 5p\rangle$, which yields four combinations (other combinations are obtained by interchanging $4p$ and $5p$):

$$\langle 5s,\epsilon p|\hat{U}|5p,\epsilon s\rangle\langle \epsilon s|\hat{D}|4p\rangle, \tag{7}$$

$$\langle 5s,\epsilon f|\hat{U}|5p,\epsilon s\rangle\langle \epsilon s|\hat{D}|4p\rangle, \tag{8}$$

$$\langle 5s,\epsilon p|\hat{U}|5p,\epsilon d\rangle\langle \epsilon d|\hat{D}|4p\rangle, \tag{9}$$

$$\langle 5s,\epsilon f|\hat{U}|5p,\epsilon d\rangle\langle \epsilon d|\hat{D}|4p\rangle. \tag{10}$$

Equations (7)–(10) show that including the virtual Auger channel in the description of conjugate satellites, a second continuum wave, namely the f wave, becomes possible, providing nonzero LMDAD from Eq. (4). The angular momentum algebra (see, e.g., Ref. [6]) and numerical calculation of matrix elements in Eq. (6) is, however, a very cumbersome task deserving an article of its own and is therefore left for the future. The discussion above, however, indicates that the description of conjugate transitions with two partial waves with different orbital angular momenta is theoretically feasible, providing a qualitative understanding for the present experimental results.

V. CONCLUSIONS

LMDAD of photoionization satellites of atomic Rb was studied experimentally. The data were used to study dynamics and symmetries of continuum waves of satellite transitions. MSU transitions can be understood and described using the sudden approximation, and more importantly it breaks down in the description of conjugate satellite transitions. The result is important for theoretical understanding of conjugate transitions. It was also shown that LMDAD is a very sensitive probe of electron correlations and especially continuum interactions. The experimental data are of very high quality and can be effectively used to test theoretical models. A model based on the perturbation theory for the conjugate transitions that may explain the experimental results was discussed.

ACKNOWLEDGMENTS

For financial support K.J. thanks the Research Council for Natural Sciences and Engineering of the Academy of Finland. The assistance of the Elettra staff during the course of the experiments is gratefully acknowledged.

[1] T. Åberg, Phys. Rev. **156**, 35 (1967).
[2] T. Åberg, Phys. Lett. **26**, 515 (1968).
[3] F. Wuilleumier and M. O. Krause, Phys. Rev. A **10**, 242 (1974).
[4] T. Ishihara, J. Mizuno, and T. Watanabe, Phys. Rev. A **22**, 1552 (1980).
[5] J. E. Hansen and P. Scott, Phys. Rev. A **33**, 3133 (1986).
[6] T. M. Luke, J. D. Talman, H. Aksela, and M. Leväsalmi, Phys. Rev. A **41**, 1350 (1990).
[7] B. Langer, J. Viefhaus, O. Hemmers, A. Menzel, R. Wehlitz, and U. Becker, Phys. Rev. A **43**, 1652 (1991).
[8] G. B. Armen and F. P. Larkins, J. Phys. B **24**, 2675 (1991).
[9] V. Schmidt, Rep. Prog. Phys. **55**, 1483 (1992).
[10] J. C. Liu, Z. W. Liu, and H. P. Kelly, Phys. Rev. A **50**, 3909 (1994).
[11] U. Becker and D. A. Shirley (editors), *VUV and Soft X-ray Photoionization* (Plenum, New York, 1996).
[12] W. T. Cheng, E. Kukk, D. Cubaynes, J.-C. Chang, G. Snell, J. D. Bozek, F. J. Wuilleumier, and N. Berrah, Phys. Rev. A **62**, 062509 (2000).
[13] G. Snell, M. Martins, E. Kukk, W. T. Cheng, and N. Berrah, Phys. Rev. A **63**, 062715 (2001).
[14] K. Jänkälä, J. Schulz, and H. Aksela, J. Electron Spectrosc. Relat. Phenom. **161**, 95 (2007).
[15] D. Cubaynes, E. Heinecke, T. Richter, S. Diehl, F. J. Wuilleumier, P. Zimmermann, and M. Meyer, Phys. Rev. Lett. **99**, 213004 (2007).
[16] S. Fritzsche, K. Jänkälä, M. Huttula, S. Urpelainen, and H. Aksela, Phys. Rev. A **78**, 032514 (2008).
[17] E. G. Drukarev, E. Z. Liverts, M. Ya. Amusia, R. Krivec, and V. B. Mandelzweig, Phys. Rev. A **77**, 012715 (2008).
[18] V. G. Yarzhemsky, M. Ya. Amusia, P. Bolognesi, and L. Avaldi, J. Phys. B **43**, 185204 (2010).
[19] M. Meyer, A. N. Grum-Grzhimailo, D. Cubaynes, Z. Felfli, E. Heinecke, S. T. Manson, and P. Zimmermann, Phys. Rev. Lett. **107**, 213001 (2011).
[20] K. Jänkälä, S. Fritzsche, M. Huttula, J. Schulz, S. Urpelainen, S. Heinäsmäki, S. Aksela, and H. Aksela, J. Phys. B **40**, 3435 (2007).
[21] D. Cubaynes *et al.*, Phys. Rev. Lett. **77**, 2194 (1996).
[22] L. Vo Ky, P. Faucher, A. Hibbert, J.-M. Li, Y.-Z. Qu, J. Yan, J. C. Chang, and F. Bely-Dubau, Phys. Rev. A **57**, 1045 (1998).
[23] V. V. Balashov, A. N. Grum-Grzhimailo, and N. M. Kabachnik, *Polarization and Correlation Phenomena in Atomic Collisions* (Kluwer Academic/Plenum, New York, 2000).
[24] F. J. Wuilleumier and M. Meyer, J. Phys. B **39**, R425 (2006).

[25] M. Meyer, Nucl. Instrum. Methods Phys. Res., Sect. A **601**, 88 (2009).
[26] A. N. Grum-Grzhimailo and M. Meyer, Eur. Phys. J. Spec. Top. **169**, 43 (2009).
[27] A. von dem Borne, T. Dohrmann, A. Verweyen, B. Sonntag, K. Godehusen, and P. Zimmermann, Phys. Rev. Lett. **78**, 4019 (1997).
[28] K. Godehusen, P. Zimmermann, A. Verweyen, A. von dem Borne, Ph. Wernet, and B. Sonntag, Phys. Rev. A **58**, R3371 (1998).
[29] Ph. Wernet, J. Schulz, B. Sonntag, K. Godehusen, P. Zimmermann, A. N. Grum-Grzhimailo, N. M. Kabachnik, and M. Martins, Phys. Rev. A **64**, 042707 (2001).
[30] J. Schulz, Ph. Wernet, K. Godehusen, R. Müller, P. Zimmermann, M. Martins, and B. Sonntag, J. Phys. B **35**, 907 (2002).
[31] A. N. Grum-Grzhimailo, J. Phys. B **34**, L359 (2001).
[32] J. Niskanen, S. Urpelainen, K. Jänkälä, J. Schulz, S. Heinäsmäki, S. Fritzsche, N. M. Kabachnik, S. Aksela, and H. Aksela, Phys. Rev. A **81**, 013406 (2010).
[33] J. Schulz, M. Tchaplyguine, T. Rander, O. Björneholm, S. Svensson, R. Sankari, S. Heinäsmäki, H. Aksela, S. Aksela, and E. Kukk, Phys. Rev. A **72**, 010702 (2005).
[34] R. R. Blyth *et al.*, J. Electron Spectrosc. Relat. Phenom. **103**, 959 (1999).
[35] National Institute of Standards and Technology (NIST), Atomic Spectra Database Energy Levels [http://physics.nist.gov/PhysRefData/ASD/].
[36] A. Moise, M. Alagia, L. Banchi, M. Ferianis, K. C. Prince, and R. Richter, Nucl. Instrum. Methods Phys. Res., Sect. A **588**, 502 (2008).
[37] A. Moise, M. Alagia, L. Avaldi, V. Feyer, K. C. Prince, and R. Richter, J. Phys. B **43**, 215001 (2010).
[38] S. Baier, A. N. Grum-Grzhimailo, and N. M. Kabachnik, J. Phys. B **27**, 3363 (1994).
[39] A. Verweyen, A. N. Grum-Grzhimailo, and N. M. Kabachnik, Phys. Rev. A **60**, 2076 (1999).
[40] R. D. Cowan, *The Theory of Atomic Structure and Spectra* (University of California Press, Berkeley, 1981).
[41] T. N. Chang and R. T. Poe, Phys. Rev. A **12**, 1432 (1975).
[42] K. I. Hino, T. Ishihara, F. Shimizu, N. Toshima, and J. H. McGuire, Phys. Rev. A **48**, 1271 (1993).
[43] T. Ishihara and R. T. Poe, Phys. Rev. A **6**, 116 (1971).